

Table of Contents: Volume 2. Technical Proposal

1. Executive Summary	1
2. Technical Narrative.....	2
2.1 Overview	2
2.2 Mission Relevance.....	4
2.3 Previous Work	5
2.4 Exploiting EGFs for Event Location: The Idea	8
2.5 Exploiting EGFs for Event Location: Proof-of-Concept Results	12
2.6 Proposed Results.....	15
2.7 Benefits of the Teaming Effort Between CU-B and LLNL.....	18
2.8 Facilities.....	18
2.9 On Potential Risks and Duplication of Effort.....	18
2.10 References	19
3. Work Plan (Statement of Work).....	21
3.1 Objective	24
3.2 Background	24
3.3 Approach	24
3.4 Key deliverables.....	25
3.5 Tasks	25
3.6 Technical Role and Contributions of Team Members	25
4. Proposed Schedule	26
5. Key Personnel (Curriculum Vitae).....	27

Volume 2. Technical Proposal

Application of Empirical Green's Functions from Ambient Seismic Noise to Improve Regional Locations

Michael H. Ritzwoller (PI)
Mikhail P. Barmin (co-PI)
Center for Imaging the Earth's Interior
Department of Physics
University of Colorado at Boulder

Steven Myers (co-PI)
Lawrence Livermore National Laboratory

1. Executive Summary

This proposal responds to NNSA/AFRL/SMDC Broad Agency Announcement for Fiscal Year 2008 regarding nuclear explosion monitoring research and engineering (Solicitation Number DE-SC52-07NA28103). The proposal particularly responds to Research Topic 1: Detection, Location, Discrimination, and Yield Estimation, Subtopic 1c: Location Techniques.

There are XXXX principal deliverables:

2. Technical Narrative

2.1 Overview

This proposal responds to NNSA/AFRL/SMDC Broad Agency Announcement for Fiscal Year 2008 regarding nuclear explosion monitoring research and engineering (Solicitation Number DE-SC52-07NA28103). The proposal particularly responds to Research Topic 1: Detection, Location, Discrimination, and Yield Estimation, Subtopic 1c: Location Techniques.

The proposed research is to develop a new method of regional seismic event detection and location whose strengths and limitations complement existing location methods. This novel technique is based on exploiting Empirical Green's Functions (EGF) that are produced using ambient noise methods. Example EGFs are shown in Figure 1a,b. Elastic EGFs between pairs of seismic stations are determined by cross-correlating ambient noise time-series recorded at the two stations. We propose to develop and test new methods to produce a geographic grid of EGF's which can be used to detect and locate events accurately using waveform correlation. Because the EGF's contain the full 3-D structural response of the Earth, this method is tantamount to using an exceptionally accurate 3-D model for detection and location. Because the method is empirical, however, location error is expected to be unbiased. Furthermore, ambient noise is generated at Earth's surface, so the EGFs are necessarily for surface-focus events and are, therefore, ideal for detecting and locating human-made events.

The idea of the method is straightforward. We assume first that there is a temporary dense local array, termed the *Base Stations*, deployed in the "region of interest" where seismic events may occur. Second, there is a more distant permanent (but sparse) regional network of stations termed the *Remote Stations*. This lay-out is depicted schematically in Figure 2. Using what are now well established methods, the EGFs from every Base to Remote station are computed and are used to develop a geographic grid of EGFs from the region of interest to each of the remote stations. These grids of EGFs are then used to locate events within the region of interest using waveform correlation. Examples of this method are presented in sections 2.4 - 2.5.

One of the most significant aspects of this method is that the Base Stations do not have to be installed when the event of interest occurs. A temporary deployment of Base Stations will produce the EGFs for a grid of points in the region to each of the remote stations. Thus, when an interesting event occurs, observations of the event are only needed at the remote stations, which are assumed to be permanent. Although the longer the Base Stations can be operated the better, because longer time series produce higher signal-to-noise ratio (SNR) EGFs, quite short deployments can produce surprisingly good EGFs at periods below about 15 sec. Figure 1c,d illustrates how SNR grows with time-series length. One month of data

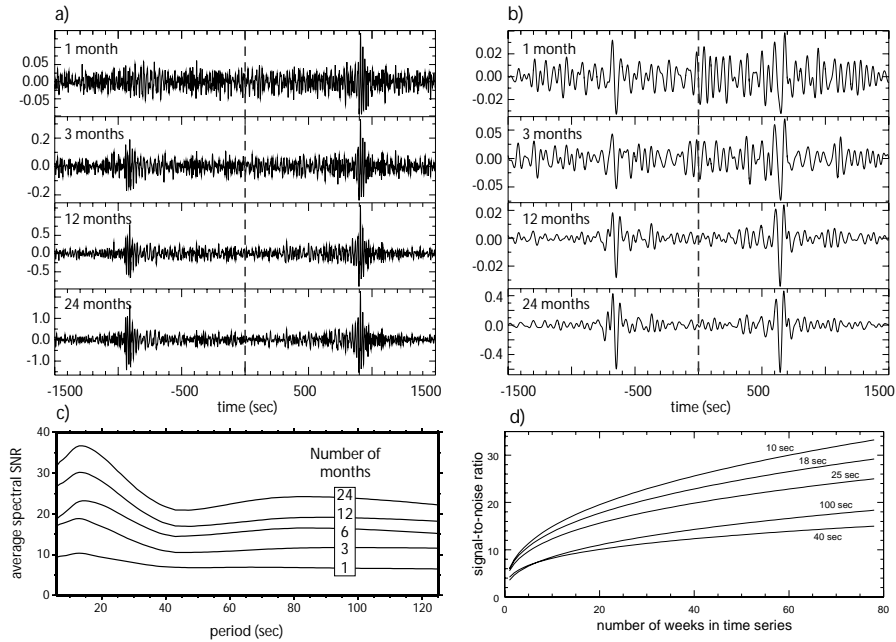


Figure 1: **Dependence of ambient noise cross-correlations on time-series length.** (a) Example vertical-vertical (Rayleigh wave) cross-correlations for different time-series lengths between the stations ANMO (Albuquerque, NM) and DWPF (Disney Wilderness, FL), band-pass filtered between 5 and 40 sec period. The positive lag (waves from ANMO to DWPF) and negative lag (waves from DWPF from ANMO) of the cross-correlation are shown. (b) Same as (a), but filtered from 40 to 100 sec period. (c) SNR versus period averaged across cross-correlations for more than 200 stations within the continental US. The lines are for four time-series lengths ranging from 1 month to 2 years. (d) SNR versus time-series length is seen to follow a power-law curve, but different curves characterize different periods. (Results are taken from Bensen et al. (2007a).)

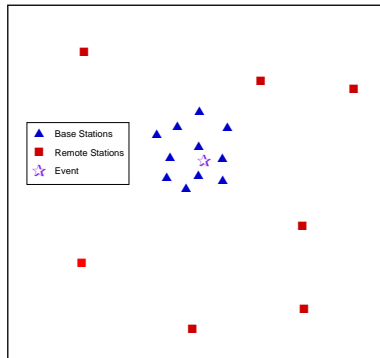


Figure 2: **Schematic observational setting.** A relatively dense set of temporary “Base Stations” (blue triangles) encompass the source region of interest (event denoted by the star). A sparse set of permanent “Remote Stations” lie farther from the region of interest.

can produce meaningful EGFs below ~ 15 sec period.

We propose to continue to improve this location method and the error analysis, test and calibrate it in several source regions where there are Ground Truth (GT) events but which have very different propagation characteristics and different observing conditions (western US, Turkey, Kirghizstan), and extend the method. At present, the method is based on using only the envelopes of the EGFs and the event data. This amounts to exploiting only wave group characteristics in the the location method, and phase information is ignored. The proposed extensions of the method will concentrate on applying phase information, which significantly complicates the technique but will have the benefit of providing other source characteristics such as the frequency-dependent radiation pattern and possibly source depth.

2.2 Mission Relevance

The proposed research aims to test and continue the development of a new location procedure based on Empirical Green's Functions (EGFs) determined from ambient noise. The proof-of-concept exercise that tests the preliminary version of the method is shown (section 2.5 below) to be very promising. This method has several characteristics that will help to advance national technical means to detect, locate, and identify nuclear explosions.

First, innovative methods are needed to improve national technical capabilities in location. The proposed method, based on producing and exploiting Composite EGFs from ambient noise, is entirely novel; to the best of our knowledge never having been conceived, developed, or applied before. In fact, the use of surface waves from earthquakes, let alone from ambient noise, remains a frontier topic that is receiving greater attention in recent years (e.g., http://mnw.eas.slu.edu/Earthquake_Center/MECH.NA).

Second, because the EGFs contain the full 3-D structural response of the Earth, this method is equivalent to using an exceptionally accurate 3-D model – the earth itself – for detection and location. Locations from the method will not be biased, therefore, due to ignorance about 3-D wave propagation effects. This complements body wave location methods based on structural models or incomplete travel time correction surfaces. Uncertainties in phase identification, which can plague regional body wave locations, also are not a problem.

Third, because ambient noise is generated at Earth's surface, the EGFs are necessarily for surface-focus events and are, therefore, ideal for detecting and locating human-made events such as explosions. The method may degrade for events deeper than the mid-crust, but it is well suited for locating shallow explosions.

Fourth, the method is designed to exploit temporary deployments of Base Stations in regions of interest. The Base Stations need not be operating during the occurrence of an event of interest. In fact, temporary deployments as short as a month may be sufficient to obtain reliable EGFs in some places, perhaps even shorter for Remote Stations that are

relatively close.

Fifth, our proof-of-concept study indicates that the preliminary error ellipses appear to capture location errors. This is an important characteristic of a reliable location method.

Finally, although the method is being developed to locate events, the Composite EGFs can be used in a straightforward way as a detector. The method also has relevance to event identification through location.

In summary, the novel location method that we propose to continue to develop, test, and apply complements the capabilities of single-event and multi-event (e.g., JHD, double-difference methods) methods that are now commonly in use and will add a new weapon in the arsenal to identify, locate, and identify seismic events.

2.3 Previous Work

The use of ambient seismic noise to perform surface wave tomography, also called ambient noise tomography (ANT), has become a well established method to estimate short period (<20 sec) and intermediate period (between 20 and 50 sec) surface wave speeds on both regional (e.g., Sabra et al., 2005b; Shapiro et al., 2005; Yao et al., 2006; Cho et al., 2007; Lin et al., 2007a; Moschetti et al., 2007; Villasenor et al., 2007) and continental (e.g., Yang et al., 2007; Bensen et al., 2007b) scales. In these studies, Rayleigh wave Empirical Green's Functions (EGFs) between station-pairs are estimated by cross-correlating long time-sequences of ambient noise recorded simultaneously at both stations. For a pair of stations A and B, the EGF is computed from the cross-correlogram between the station pairs by taking the negative time-derivative:

$$G_{AB}(t) = -\frac{1}{2}(C_{AB}(t) - C_{AB}(-t)) \quad (1)$$

where $C_{AB}(t)$ is the cross-correlogram at positive time lag and $C_{AB}(-t)$ is the cross-correlogram at negative time lag.

The studies referred to in the previous paragraph have established that, within reasonable tolerances:

- (1) the EGFs and dispersion measurements are repeatable when performed in different seasons and seasonal variability presents a useful measure of uncertainty,
- (2) the EGFs agree with the surface wave parts of shallow focus earthquakes,
- (3) the dispersion measurements agree with those received from earthquakes,
- (4) the resulting tomography maps cohere with known geological structures such as sedimentary basins and mountain ranges, and

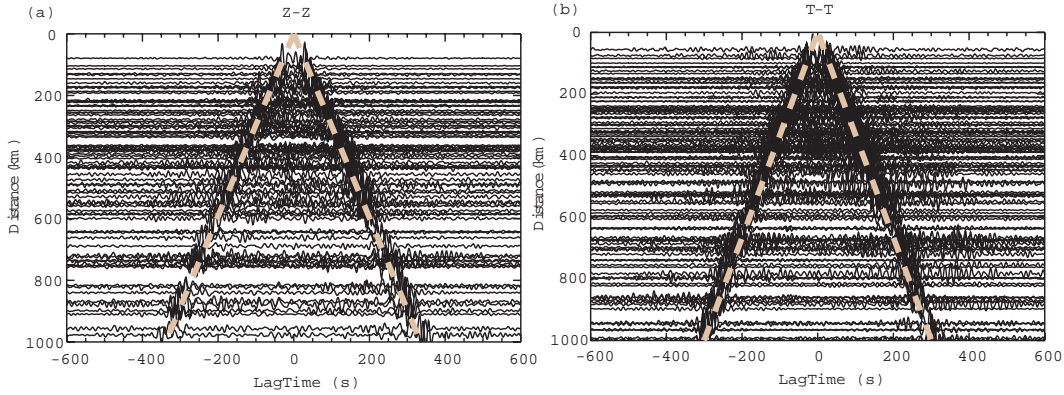


Figure 3: **Example vertical-vertical (Z-Z, Rayleigh wave) and transverse-transverse (T-T, Love wave) cross-correlation record section across the western US.** The reference station is MOD (Modoc Plateau, CA) and other stations are from the EarthScope Transportable Array. Band pass: 10 - 50 sec period. One year time-series. Reference move out: 3 km/sec for Z-Z, 3.3 km/sec for T-T. (Figure taken from Lin et al. (2007b).

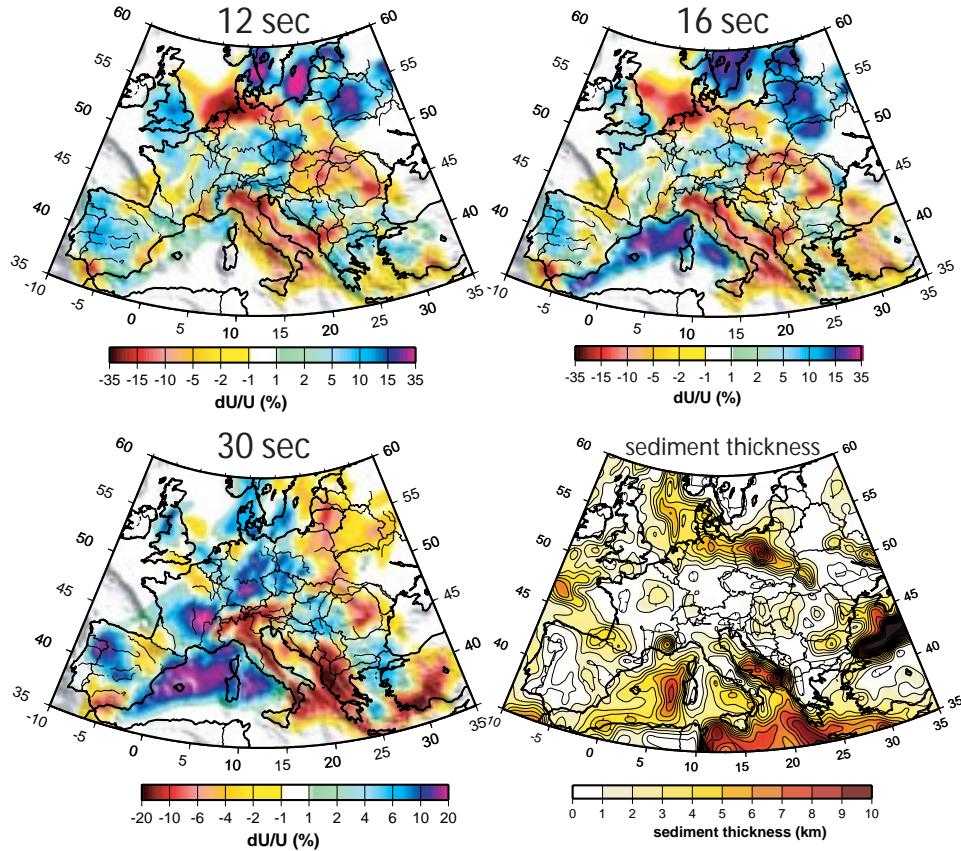


Figure 4: **Example group velocity maps across Europe.** Correlation with geological features is apparent, particularly sedimentary basins (map from Laske & Masters) at shorter periods and crustal thickness variations (e.g., Alps, Carpathians) at longer periods.

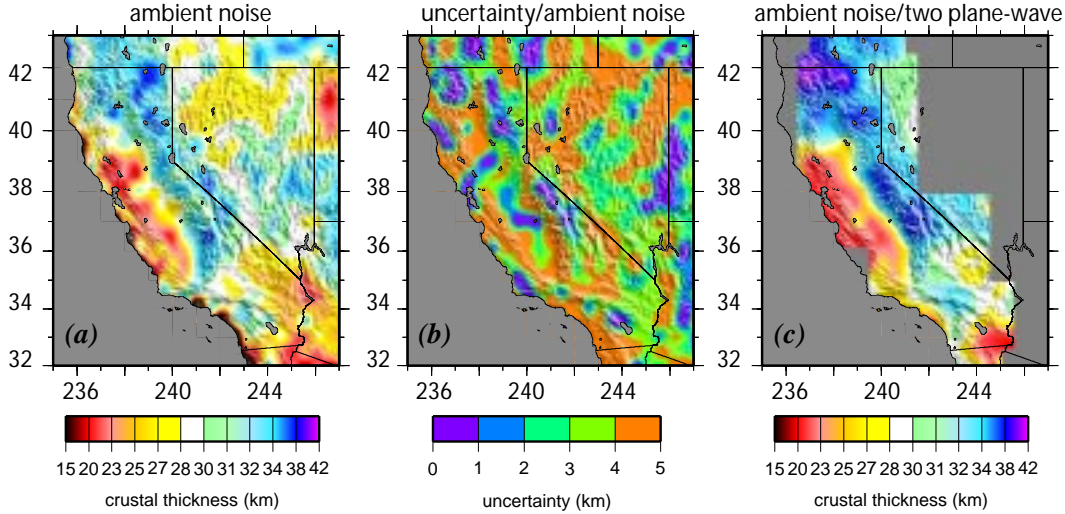


Figure 5: **Preliminary estimates of crustal thickness across California.** (a) Best fit crustal thickness from the Monte-Carlo inversion of Rayleigh wave group and phase speed curves (6 - 40 sec) obtained from ambient noise tomography. (b) Half-width of full range of Moho depths from the Monte-Carlo inversion. (c) Crustal thickness from a preliminary linearized inversion of Rayleigh wave phase speeds obtained from ambient noise (8-25 sec) and two plane-wave (30 - 150 sec) tomography (Yang and Forsyth, 2006), plotted for comparison.

- (5) the resulting tomography maps display higher resolution and are obtained to much shorter periods than those typically derived from teleseismic earthquakes.

The observational methodology underlying ambient noise dispersion analysis is described in detail by Bensen et al. (2007a). Recent observational advances include extending the ambient noise derived measurements to phase velocities (e.g., Yao et al., 2006; Lin et al., 2007b) and Love waves (Lin et al., 2007b). Figure 3 shows an example record section across the western US demonstrating both Rayleigh and Love waves.

We have applied ANT successfully in the US (Moschetti et al., 2007; Bensen et al., 2007b), Europe (Yang et al., 2007), New Zealand (Lin et al., 2007a), Spain (Villasenor et al., 2007) and more recently in South Africa and western China (unpublished). Example group velocity maps across Europe are shown in Figure 4.

Ambient noise tomography also is beginning to be used in the construction of 3-D models of the crust and uppermost mantle which exploit ANT's higher lateral resolution and extension to shorter periods than traditional single-station earthquake tomography. This results in tighter constraints on crustal structures. One example is Yoo et al.(2007). Figure 5 presents a comparison of crustal thickness across California and Nevada estimated with a Monte-Carlo inversion based on ambient noise dispersion measurements with crustal thickness from teleseismic two-plane tomography (Yang and Forsyth, 2006). This work is currently in-progress.

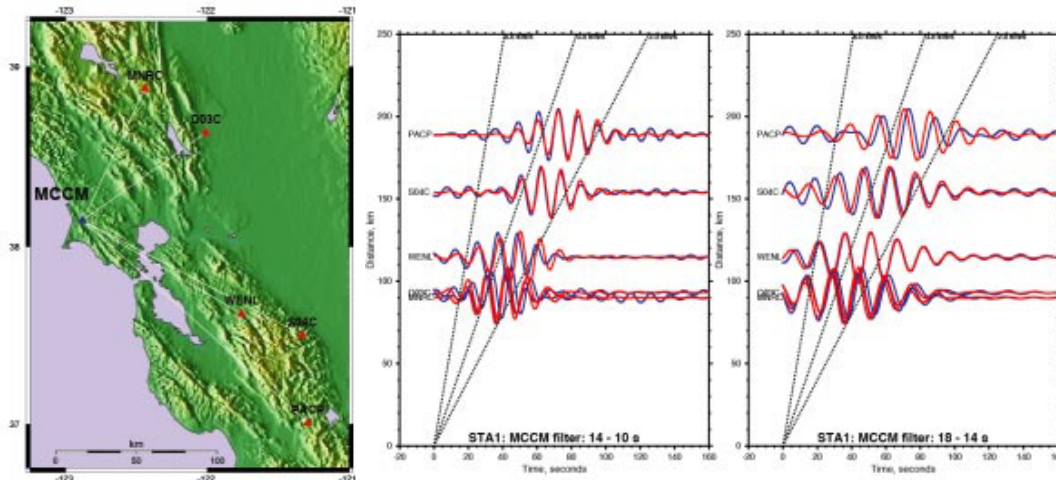


Figure 6: **Exploratory test of using Empirical Green’s Functions to calibrate the northern California community 3-D model.** (LEFT PANEL) Synthetic seismograms are computed through the 3-D model produced by a vertical impulsive force at station MCCM (Marshall, CA, near the Point Reyes Peninsula) recorded at several other broad-band stations around the Bay Area. (MIDDLE PANEL) Synthetics (red lines) are compared with the EGFs (blue lines) in the Bay Area; the band-pass filter is centered at 10 sec period. (RIGHT PANEL) Synthetics are compared with EGFs with the center of the band-pass filter at 14 sec period.

The Empirical Green’s Functions that emerge from ambient noise data processing are beginning to be used directly to validate and calibrate the northern California community 3-D model which is designed for ground shaking simulations needed in seismic hazard assessment (Rodgers et al., 2007). Observations of the general agreement between the synthetics and EGFs in the San Francisco Bay area (e.g., Fig. 6) have provided a motivation for the current proposal.

2.4 Exploiting EGFs for Event Location: The Idea

The basic idea of the use of Empirical Green’s Functions (EGFs) determined from ambient noise to locate regional events is illustrated in Figures 7-10. Preliminary results of locating Ground Truth events in California are shown in the next section and summarized in Table 1.

Consider, for example, locating an earthquake, such as the $m_b = 4.5$ event that occurred north of the San Francisco Bay area on May 12, 2006, area shown in Figure 7c. This is Earthquake 13 from Table 1. A vertical component earthquake record and a vertical-vertical EGF from a station near to the epicenter are shown in Figure 7a,b. The earthquake record is from station V04C, and the inter-station EGF is for stations GASB (about 100 km from the epicenter) and V04C. Both time-series are band-pass filtered between 7 and 15 sec period

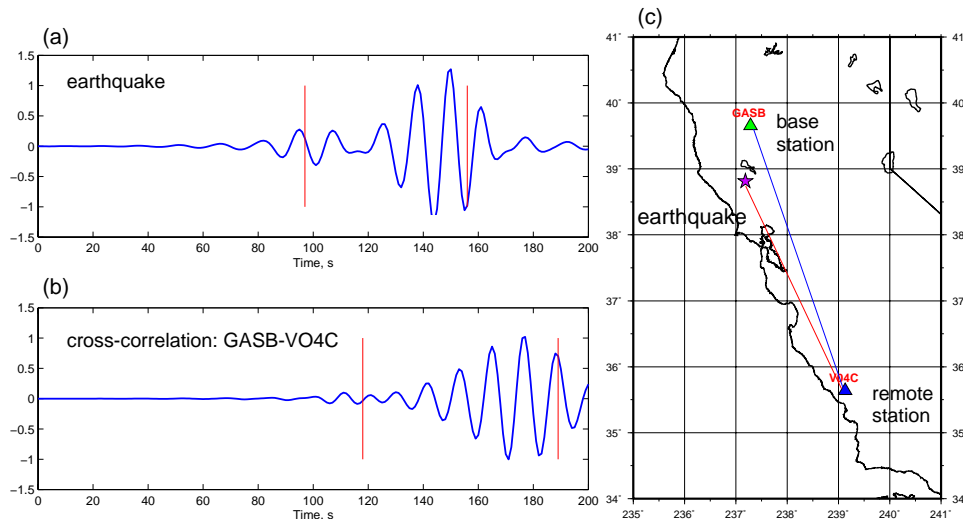


Figure 7: **Comparison of an earthquake record with an Empirical Green’s Function.** (a) Earthquake record band-passed between 7 and 15 sec period observed at station V04C in southern California. (Earthquake 13 from Table 1: May 12, 2006; 38.816N, 122.816E; $m_b = 4.5$, location from Northern California Earthquake Center). (b) EGF between stations GASB (north of the earthquake) and V04C similarly band-passed. Red lines mark 2 and 4 km/sec. (c) Location map showing earthquake and station locations.

and are dominated by the Rayleigh wave. The earthquake and EGF waveforms are similar, but are shifted in time because the epicentral distance is smaller than the inter-station distance. The EGF can be shifted in time to match the epicentral distance and deformed based on knowledge of the frequency dependence of group speed, which we have mapped in this region. The waveforms are compared in Figure 8 in which the EGF has been translated and deformed in this way to approximate its appearance if the Base Station was at the epicenter. The phase content of the the two records differs appreciably, both because of the distance difference but also because the earthquake imparts an initial phase that depends on hypocentral depth and source mechanism. For this reason, we (initially) ignore phase information and summarize both the EGFs and the earthquake records with their envelope functions, as seen in Figure 8 as dashed lines. The EGFs for each of the Base Stations relative to the Remote Station can be similarly transformed to the earthquake location and stacked to yield a **Composite EGF** for a particular source location and Remote Station, as illustrated in Figure 9. Typically, the Composite EGF agrees with the earthquake record better than the individual EGFs from the Base Stations.

The Composite EGFs for a candidate event location can be produced for all of the Remote Stations, as the record section shown in Figure 10 illustrates. Inspection of fit between the Composite EGFs and the earthquake envelope functions reveals that 3-D structure similarly affects the EGFs and the earthquake records. For example, consider the arrivals at stations HUMO, Q08A, and PHL, which are within several kilometers in epicentral distance from

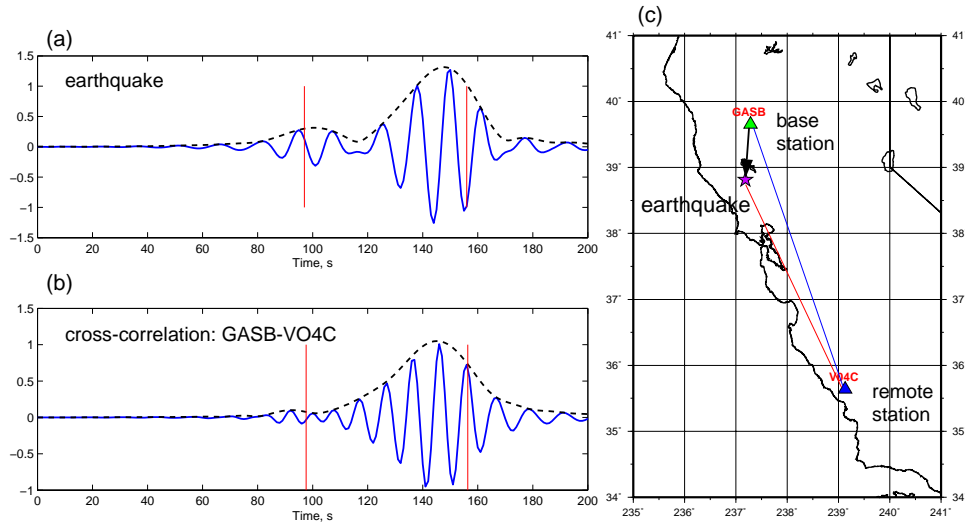


Figure 8: **Comparison of an earthquake record with an Empirical Green's Function shifted to the epicenter location.** Same as Fig. 7, but the EGS has been shifted and deformed correspond to the earthquake location. Envelope functions are shown in (a) and (b) with dashed lines.

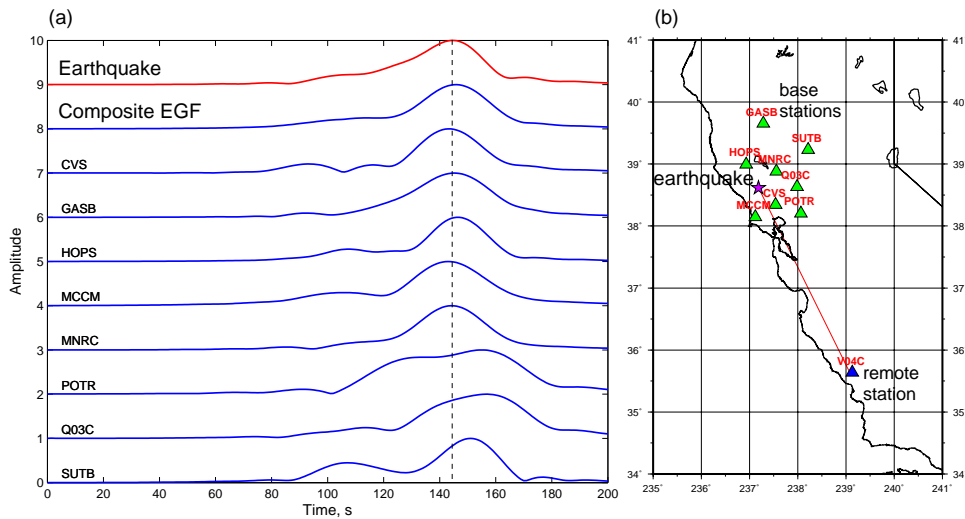


Figure 9: **Comparison of Empirical Green's Functions from the set of Base Stations.** Similar to Fig. 8, but the EGFs for the 8 base stations are shown in (a). The earthquake record is shown in red at top and the Composite EGF (stack of the individual EGFs transformed to the epicentral location) is on the second line.

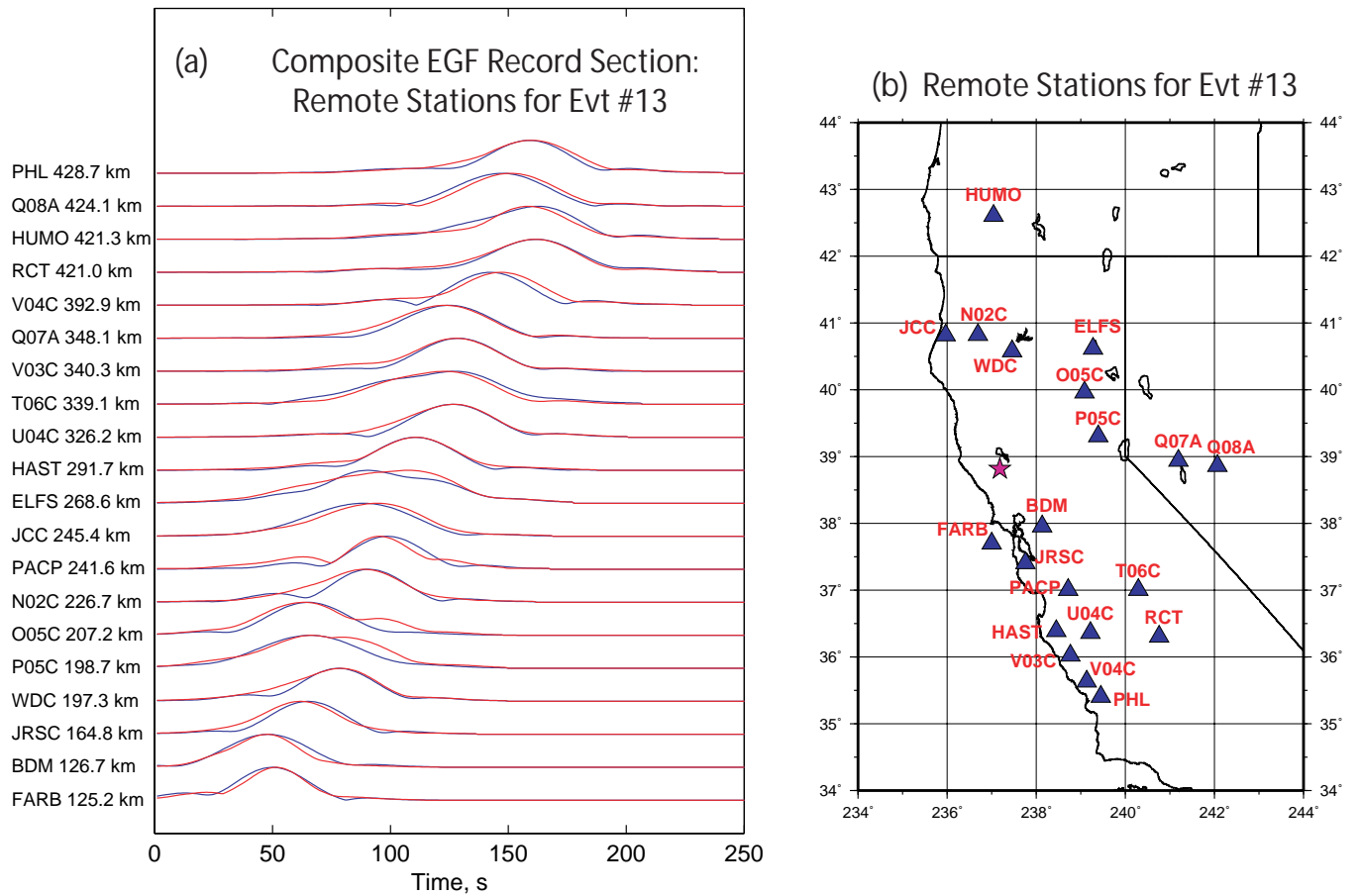


Figure 10: **Record section of the Composite Empirical Green's Functions compared with the earthquake records at 20 Remote Stations for Event #13.** (a) Envelope functions of the earthquake observed at the Remote Stations (red lines) are compared with the Composite EGFs (blue lines). Band-pass: 7-15 sec period. Earthquake characteristics are listed in Fig. 7 caption and Table 1. Epicentral distances and station names are indicated at left. (b) Locations of the Remote Stations and the earthquake. The locations of the 8 base stations are shown in Fig. 9.

each other. The Rayleigh wave arrives much earlier at Q08A than the other stations because of fast propagation through the Sierra Nevada. In fact, the fast arrivals in the record section all propagate in part through the Sierra Nevada. In addition, some of the envelope functions are significantly broader than others. Stations ELFS and T06C present examples for wave propagation across and oblique to the Great Valley sediments of central California.

2.5 Exploiting EGFs for Event Location: Proof-of-Concept Results

Table 1 presents the GT locations for 15 California earthquakes with m_b between 4.5 and 5 that occurred in 2005 and 2006. Figure 12a plots the locations of these events. There are two locations for a single event (#9 and #10), and we discard location #9 as inaccurate. All statistics are presented relative to the other locations. The location error reported in Table 1 is defined as the distance between the GT location and the location determined from our Composite EGFs described now in this section. The GT locations are determined by Cal Tech in southern California and the Northern California Earthquake Center in Menlo Park for northern California events. Both groups use a combination of broad-band and short period instruments and 1-D models calibrated for their region. Cal Tech uses both P and S, whereas only P is used in northern California. The locations for these events are believed to be better than 1 km in most cases (Egill Hauksson, James Dewey, Bob Engdahl, personal communication). This probably translates to a 90% confidence that the location is better than 2 km, making these GT2 events on average.

Table 1. Event information.

evt #	yr	mo	day	hr	min	sec	source [†]	lat	lon	m_b	Error (km)
1	2005	04	16	19	18	13.00	P	35.027	-119.178	4.9	5.0
2	2005	05	16	07	24	37.50	NC	35.929	-120.477	4.3	1.0
3	2005	06	12	15	41	46.54	P	33.529	-116.572	5.1	3.6
4	2005	06	16	20	53	26.02	P	34.058	-117.010	4.8	2.8
5	2005	06	26	18	45	57.82	NC	39.305	-120.093	4.6	2.2
6	2005	08	31	22	47	45.64	P	33.165	-115.635	4.5	5.0
7	2005	08	31	22	50	24.03	P	33.172	-115.610	4.9	5.1
8	2005	08	31	23	32	11.04	P	33.190	-115.602	4.5 (M_L)	1.0
9*	2005	09	02	01	27	18.61	P	33.175	-115.630	4.5 (M_L)	6.3
10	2005	09	02	01	27	19.81	P	33.160	-115.637	4.9	3.6
11	2005	09	22	20	24	48.62	P	35.043	-119.013	4.8	2.2
12	2005	10	02	13	48	09.45	NC	35.651	-121.087	4.5	1.0
13	2006	05	12	10	37	29.31	NC	38.816	-122.816	4.5	0.0
14	2006	06	15	12	24	51.11	NC	37.102	-121.492	4.5	2.2
15	2006	08	03	03	08	12.86	NC	38.364	-122.589	4.6	1.4

†: P – Pasadena, NC – Northern California *: – location #9 is discarded.

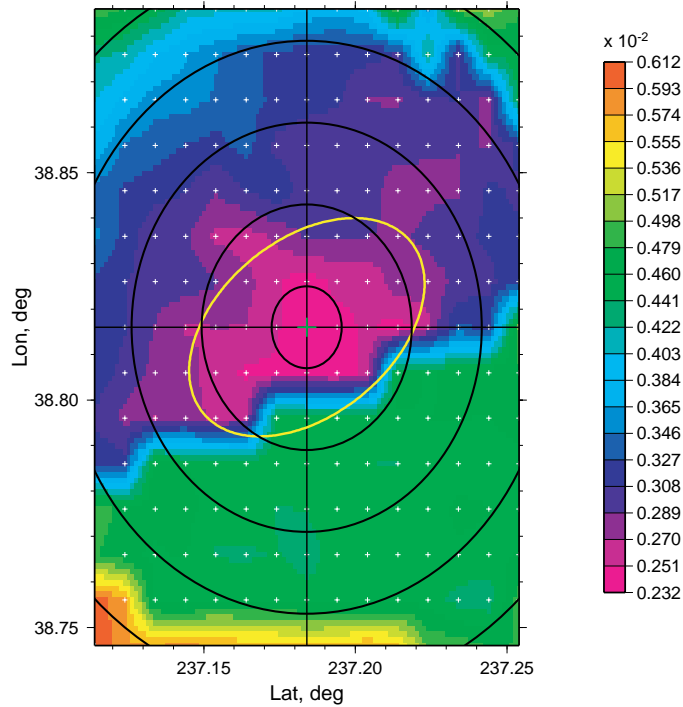


Figure 11: **Residual surface for Event 13 showing the best fit location and error ellipse.** Misfit between the Composite EGFs and the earthquake envelope functions; cool colors indicate good fit. Black cross-hairs intersect at the GT location. The best fit location is indicated with the green plus sign, coincident here with the GT location. Smaller white plus signs mark the ~ 1 km grid of hypothetical locations. Black contours denote distances of 1 km, 3 km, 5 km, etc from the GT location. The yellow error ellipse is the estimate for our location.

In the examples shown in Figures 7-10, the earthquake location is well constrained, having been located by a dense network of short period instruments by the Northern California Earthquake Center. We turn the construction of the composite EGFs into a location method by computed them on a grid of hypothetical epicentral locations and then for each location comparing with the earthquake records by waveform cross-correlation. In this case, the waveforms for both the Composite EGFs and the earthquakes are envelope functions. Misfit statistics for the Composite EGFs and the earthquake envelope functions for each point on the grid are computed for each point on the grid and the location is identified with the best-fitting grid point. Such a comparison can be done by eye using Figure 10, but in the location procedure it is done automatically by computing misfit or residual between the Composite EGFs and the earthquake envelope functions.

An example of a misfit or residual surface is shown in Figure 11 for the northern California earthquake featured in Figures 7-10 (Event 13 of Table 1). In this proof-of-concept exercise, a fairly coarse ~ 1 km grid is employed. The cross-hairs mark the GT location, which is coincident with the minimum of the residual surface and, hence, the location determined by

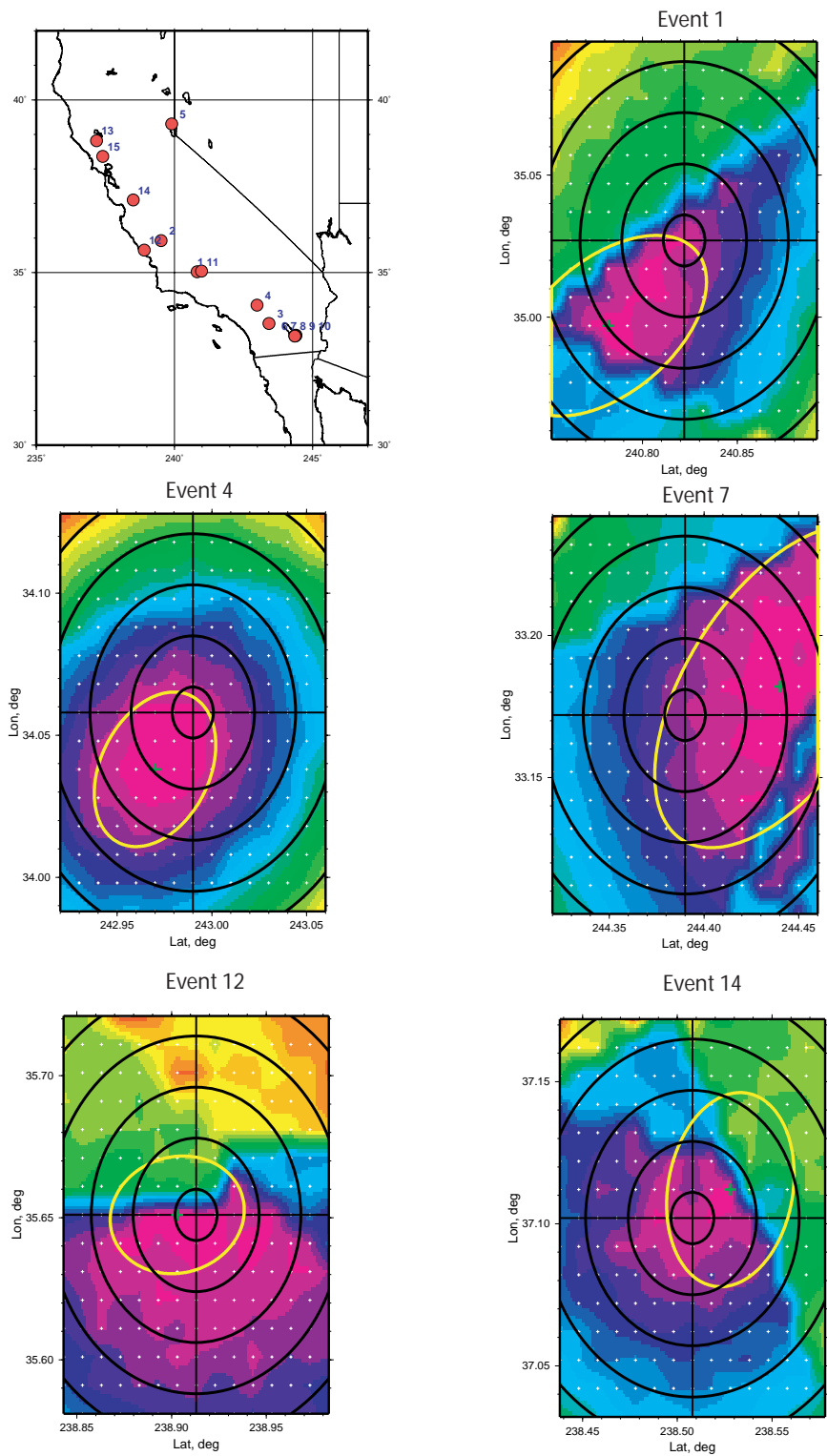


Figure 12: **Collage of residual surfaces for several events.** Event locations are numbered and shown at upper left and in Table 1. F The format of residual surfaces is described in Fig. 11.

the Composite EGFs. We have also developed a prototype error analysis which is beyond the scope of the proposal to describe except to say that is a variant of the method of Jordan and Sverdrup (1981). The estimated error ellipse for Event 13 also is shown in Figure 11. Summary location “errors” (the distance between our locations and the GT locations) for all 15 California events are presented in Table 1. Other examples of residual surfaces are shown for Events 1, 4, 7, 12, and 14 in Figure 12.

The average error for our method applied to the 15 earthquakes in Table 1 is about 2.6 km. Locations errors less than the GT level (~ 1 km) are unlikely. In comparison, the average error of the EarthScope Array Network Facility’s (ANF) location based on regional P and S travel times observed at the Transportable Array component of EarthScope is about 3.6 km. We infer from this that the proposed method appears to be as good as or can beat body wave location methods unless the body wave method (1) is tuned to local structure and (2) is based on a much denser array of stations surrounding the event as it occurs. In addition, the locations do not demonstrate systematic bias. Our mean location error is about 0.3 km north and 0.5 km east of the GT location, which is well below the average error of 2.6 km.

We view the results of this exercise to be very promising. Indeed, it would have been difficult for the locations to have agreed appreciably better with the GT events for several reasons. (1) We used 1 sps data which imparts a 0.5 sec uncertainty in the arrival times (~ 1.5 km). (2) We used a 1 km location grid which introduces another ~ 0.5 km fluctuation. (3) The GT locations are GT1-GT2 in accuracy. An average 1 km error would be theoretically possible, and its ultimate achievement is an aim of this proposal.

2.6 Proposed Research

The proposed research will break into three principals subject areas:

- (1) Continue to develop the location method based on waveform correlation between the envelope functions of Composite Empirical Green’s Functions (EGFs) determined from ambient noise and earthquake records.
- (2) Test the method in three locations with different structural and waveform effects and different array geometries and characteristics.
- (3) Extend the method to incorporate phase information.

2.6.1 Continued Method Development

The results presented above in sections 2.4-2.5 are based on many details that have not been described here which together can be viewed as parameters that define the method. We need

to explore these parameters in a systematic way to help us understand the method better and also to provide the means to tweak the method in different observational settings.

The parameters that define the current method include, but are not limited to, choices related to (a) the frequency band used, (b) the distance ranges that define the Base Stations and Remote Stations, (c) the group velocity window applied prior to waveform cross-correlation, and (d) the time-series sampling rate. The choices here are (a) 7 - 15 sec period, (b) Base Stations are at distances < 100 km and Remote Stations from 100 to 400 km, (c) 2.5 - 4.0 km/sec, and (d) 1 sps. Although these choices have not been made arbitrarily, we have not yet explored systematically the effect on the method of varying each of these parameters. In particular, the definition of Base and Remote stations worked well in California but would be impractical in many regions of the world in which Base Stations and Remote stations may be separated by greater distances. In addition, the use of both higher frequency and lower frequency waves may help the method in some cases and we need to explore this carefully. The use of higher frequencies will require that data with a higher sampling rate than 1 sps be used in the ambient noise data processing.

In addition, we have made a set of algorithmic choices in transforming each station EGF to a hypothetical event location, in normalizing the amplitude spectrum of the EGF and earthquake records, and stacking the EGFs to produce the Composite EGF, and in performing the waveform correlation. The algorithm itself requires further scrutiny and tuning to begin to reach an operational level.

In each of these cases, research is focused on the ability to produce Composite Empirical Green's Functions on an arbitrary grid of hypothetical event locations encompassed by a set of Base Stations with various inter-station distances observed at a set of Remote Stations at various distances. Examples of the output of the current algorithm are shown in Figure 10.

Two other developments are needed in addition to systematic exploration of the parameters that define the method and continued development of the algorithm. First, the preliminary error analysis that produces the error ellipses shown in Figures 11 and 12 needs to be tested further and potentially improved. Second, all analysis presented here has been based on cross-correlations of ambient noise recorded on vertical components, so only Rayleigh waves have been observed. Lin et al. (2007b) have demonstrated the ubiquity of Love waves in ambient noise, and they can be exploited, too. We also propose to investigate incorporating them in the location procedure.

Most of this work will be completed in Year 1 and the first part of Year 2 of the proposed research.

2.6.2 Observational Tests in a Variety of Settings

We propose to continue to test the location method using GT events in the western US, Turkey, and Kirghizstan. These locations and observing networks provide a variety of settings and different challenges and obstacles in which to test the location method.

In the US, we will continue to locate events that have been located accurately by regional networks such as Cal Tech and the Northern California Earthquake Center performed here. The basis for this work will be the Transportable Array (TA) component of EarthScope/USArray which is currently sweeping across the US with an inter-station spacing of about 70 km. The TA is currently built-out in California, Oregon, Washington, Idaho, and Nevada, and is fractionally installed in Arizona, Utah, and Montana. The size and uniform spacing of this network together with its geographical expanse provide a great many settings with which to test the method. This control is ideal in the early stages of the development of the algorithm. These tests will be completed late in Year 1 and early in Year 2 of the proposed research.

We seek tests of the method outside the US, however, and propose to perform them in two regions: Turkey and Kirghizstan. In both regions, Remote Stations are fewer in number, separated from the Base Stations by longer distances, and more sparsely distributed than in the US. We anticipate that this will place strong constraints on the method, perhaps requiring that the method be extended to longer periods, for example. In both cases, Base Stations will be separated by considerably greater distances than in the examples presented in California in the foregoing. This will make the production of the Composite EGFs more dependent on knowledge of local dispersion characteristics as individual EGFs will need to be translated over larger distances. In our view, this challenge provides an excellent focus for the proposed research.

In Turkey, we will use data from the North Anatolian Fault PASSCAL experiment operated by Prof. Sue Beck and collaborators. Prof. Beck has agreed to provide early access to these data via the IRIS DMC. This 40 station array straddles the North Anatolian fault in central Turkey. Well located events within the footprint of the array will be relocated using the Composite EGF method using Remote Stations throughout the Near East and Middle East. In Kirghizstan, we will use the KNET stations as Base Stations and Remote Stations throughout Central Asia. GT locations will be supplied by the Kirghiz Institute of Seismology in Bishkek. Dr. Tamara Sabitova is the contact there, and has agreed to work with us on this project. She is Anatoli Levshin's ex-graduate student, so we have good lines of communication with her.

Tests in Turkey and Kirghizstan will be completed late in Year 2 and in Year 3 of the proposed research.

2.6.3 Extending the Method

The third and final proposed subject involves extending the method to incorporate phase information. This is desirable because observations of phase arrival times are much more regular than group times, as waveform envelopes are a less stable observable than phases. At the outset, this advantage is offset by the dependence of the earthquake phase on source depth and radiation pattern, which means that for phase information to be used the frequency dependence of the radiation pattern has to be estimated in addition to the earthquake location. This complicates the analysis, but is worth pursuing because phase information may improve the event location considerably. This will need to be determined, however. We propose to extend the method to incorporate phase information by estimating location and the frequency-dependent azimuthal radiation pattern simultaneously. This part of the research will be conducted in Year 3, and is seen as exploratory in nature.

2.7 Benefits of the Teaming Effort: Collaboration between CU-Boulder and LLNL

DESCRIBE ROLE OF STEVE MYERS.....

2.8 Facilities

The resources needed to complete the proposed research are largely computational. The proposed work will be carried out using the computing center at the Center for Imaging the Earth's Interior (CIEI). This is an up-to-date facility that includes two multiprocessor file servers from Sun Microsystems, numerous Sun and Linux workstations, several PC linux clusters, and an assortment of stand-alone PCs and Apple Macintoshes. The center maintains disk RAID's and storage proportionate to its needs totaling at least 10 Tb. Other peripherals for tape back-up, plotting, scanning, etc. are also in place. The facility is upgraded on a regular basis to meet the growing needs of its users.

2.9 On Potential Risks and Duplication of Effort

The proposed location method is based on the use of Empirical Green's Functions determined from ambient noise. This method is entirely innovative, and there is little risk of duplication of effort at this point. The proof-of-concept location exercise presented in section 2.5 establishes that the method shows great promise to improve location capabilities when a temporary array can be deployed in a region of interest. Because the characteristics

of this new location method complement the strengths and weaknesses of existing methods, potential risks of the research is low.

2.10 References (links to CU-B papers: <http://ciei.colorado.edu/ritzwoller>)

- Bensen, G.D., M.H. Ritzwoller, M.P. Barmin, A.L. Levshin, F. Lin, M.P. Moschetti, N.M. Shapiro, and Y. Yang, Processing seismic ambient noise data to obtain reliable broadband surface wave dispersion measurements, *Geophys. J. Int.*, in press, 2007a. (<http://ciei.colorado.edu/pubs/2007/2.pdf>)
- Bensen, G.D., M.H. Ritzwoller, and N.M. Shapiro, Broad-band ambient noise surface wave tomography across the United States, in preparation 2007b.
- Cho, K. H., R. B. Herrmann, C. J. Ammon and K. Lee, Imaging the upper crust of the Korean Peninsula by surface-wave tomography, *Bull. Seism. Soc. Am.*, 97, 198-207, 2007.
- Jordan, T.H. and K.A. Sverdrup, Teleseismic location techniques and their application to earthquake clusters in the south-central Pacific, *Bull. Seism. Soc. Am.*, 71, 1105-1130, 1981.
- Lin, F., M.H. Ritzwoller, J. Townend, M. Savage, S. Bannister, Ambient noise Rayleigh wave tomography of New Zealand, *Geophys. J. Int.*, in press, 2007a. (<http://ciei.colorado.edu/pubs/2006/7.pdf>)
- Lin, F., M.P. Moschetti, and M.H. Ritzwoller, Surface wave tomography of the western United States from ambient seismic noise: Rayleigh and Love wave phase velocity maps, *Geophys. J. Int.*, submitted, 2007b.
- Moschetti, M.P., M.H. Ritzwoller, and N.M. Shapiro, Surface wave tomography of the western United States from ambient seismic noise: Rayleigh wave group velocity maps, *Geochem., Geophys., Geosys.*, submitted, 2007. (<http://ciei.colorado.edu/pubs/2007/5.pdf>)
- Pasyanos, M.E., M.H. Ritzwoller, Y. Yang, R.M. Richmond, and M.P. Moschetti, An assessment of the compatibility of event-based and noise-based dispersion measurements, Seismological Society of America, Annual Meeting, Acapulco, Mexico, April, 2007.
- Ritzwoller, M.H. and A.L. Levshin, Eurasian surface wave tomography: Group velocities, *J. Geophys. Res.*, 103, 4839-4878, 1998.
- Ritzwoller, M.H., A.L. Levshin, L.I. Ratnikova, Intermediate period group velocity maps across Central Asia, Western China, and parts of the Middle East, *Geophys. J. Int.*, 134, 315-328, 1998.
- Ritzwoller, M.H., N.M. Shapiro, M.P. Barmin, and A.L. Levshin, Global surface wave diffraction tomography, *J. Geophys. Res.*, 107(B12), 2335, 2002.
- Ritzwoller, M.H., N.M. Shapiro, A.L. Levshin, E.A. Bergman, and E.R. Engdahl, The ability of a global 3-D model to locate regional events, *J. Geophys. Res.* 108(B7), 2353, ESE 9-1 - ESE 9-24, 2003.
- Rodgers, A., M.P. Moschetti, and M.H. Ritzwoller, Application of Empirical Green's Functions from ambient noise cross-correlation to evaluate and improve high resolution

- 3-D seismic velocity models: An exploratory study for the San Francisco Bay area, Seismological Society of America, Annual Meeting, Acapulco, Mexico, April, 2007.
- Sabra, K.G., P. Gerstoft, P. Roux, W.A. Kuperman, and M.C. Fehler, Extracting time-domain Green's function estimates from ambient seismic noise, *Geophys. Res. Lett.* 32, doi:10.1029/2004GL021862, 2005a.
- Sabra, K.G., P. Gerstoft, P. Roux, W.A. Kuperman, and M.C. Fehler, Surface wave tomography from microseisms in Southern California, *Geophys. Res. Lett.*, 2005b.
- Shapiro, N.M. and M.H. Ritzwoller, Monte-Carlo inversion for a global shear velocity model of the crust and upper mantle, *Geophys. J. Int.*, 151, 88-105, 2002.
- Shapiro, N.M. and M. Campillo, Emergence of broadband Rayleigh waves from correlations of the ambient seismic noise, *Geophys. Res. Lett.*, 31, L07614, doi:10.1029/2004GL019491, 2004.
- Shapiro, N.M. M. Campillo, L. Stehly, and M.H. Ritzwoller, High resolution surface wave tomography from ambient seismic noise, *Science*, 307(5715), 1615-1618, 11 March 2005.
- Sniieder, R., Extracting the Green's function from the correlation of coda waves: A derivation based on stationary phase, *Phys. rev. E*, 69, 046610, 2004.
- Villaseñor, A., Y. Yang, M.H. Ritzwoller, and J. Gallart, Ambient noise surface wave tomography of the Iberian Peninsula: Implications for shallow seismic structure, *Geophys. Res. Lett.*, in press, 2007.
(<http://ciei.colorado.edu/pubs/2007/4.pdf>)
- Weaver, R.L. and O.I. Lobkis, On the emergence of the Green's function in the correlations of a diffuse field, *J. Acoust. Soc. Am.*, 110, 3011-3017 2001.
- Yang, Y, and D.W. Forsyth, Rayleigh wave phase velocities, small-scale convection and azimuthal anisotropy beneath southern California, *J. Geophys. Res.*, 111, B07306, doi:10.1029/2005JB004180, 2006.
- Yang, Y., M.H. Ritzwoller, A.L. Levshin, and N.M. Shapiro, Ambient noise Rayleigh wave tomography across Europe, *Geophys. J. Int.*, 168(1), page 259, 2007.
- Yao, H., Van der Hilst, R.D., and De Hoop, M.V., Surface-wave array tomography in SE Tibet from ambient seismic noise and two-station analysis: I - Phase velocity maps, *Geophys. J. Int.*, 166, p. 732-744, doi: 10.1111/j.1365-246X.2006.03028.x, 2006.
- Yoo, H. J., R. B. Herrmann, K. H. Cho and K. Lee, Imaging the three-dimensional crust of the Korean Peninsula by joint inversion of surface-wave dispersion and teleseismic receiver functions, *Bull. Seism. Soc. Am.* 97, in press, 2007.